Development of Hydraulic Fractures and Conductivity near a Wellbore

Xi Zhang and Robert G. Jeffrey*

CSIRO Earth Science and Resource Engineering, Melbourne VIC, Australia

ABSTRACT

Hydraulic fractures play an important role in establishing a high conductive pathway connecting the wellbore and reservoir. The near-wellbore fracture development is crucial to the efficiency of a fracture treatment as a smooth fracture path will reduce the flow impedance. A numerical model is used to simulate the propagation pathways followed by hydraulic fractures, in the presence of a pressurised well and natural fractures. By including the coupling of viscous fluid flow and rock deformation in the analysis, we find that the non-uniform pressure distribution along the fractures and the removal of near-well fracture closure result in growth of a fracture with less curvature (a measure of tortuosity) in its path. Moreover, the fracture curvature can be characterised by two dimensionless parameters. If multiple fractures coexist, fracture linkage is possible due to mechanical interaction between fractures, pre-existing natural fractures and the wellbore. Natural fractures can alter the hydraulic fracture propagation direction, can offset the fracture path and can provide sites for new fracture growth. In the case of two hydraulic fractures initially growing in opposite directions from the wellbore, the interaction with a natural fracture on one side of the well will result in the other fracture wing propagating faster. The complexity of the near-wellbore fracture geometry can be studied with the aid of our numerical model.

Keywords: Near-well fracture tortuosity, coupling mechanisms, naturally fractured reservoir, numerical modelling

INTRODUCTION

Multiple subparallel fractures can be generated near the wellbore because of fracture initiation from perforations spaced along and phased around the wellbore or from natural fractures and flaws that are usually not aligned with the far-field stress direction. Fractures initiated from these defects will reorient themselves to a plane perpendicular to the minimum far-field stress direction as they grow away from the wellbore. The overall result of such a fracture initiation process produces near-wellbore fracture tortuosity. As a consequence, the net pressure required to extend the fractures is increased considerably. Because of its importance to optimisation of fracture treatments, the study on this subject has continued for several decades (Hamison and Fairhurst, 1970; Daneshy, 1973; Weng, 1993; Soliman et al. 2008; Cherny et al. 2009).

Geomechanical models are of significant value in treating these sorts of problems that relate to competing fracture growth, including local width restrictions and increased viscous frictional pressure loss. Based on such geomechanical analyses, various operational remedial techniques have been proposed to overcome or avoid the near-wellbore effects, such as using higher injection rates, higher viscosity fluids and orienting slots or perforations for fracture initiation (Manrique and Venkitaraman, 2001; Abass, et al., 2009). However, most studies were based on the uniform pressurization assumption so that the fracture problem can be treated by conventional fracture mechanics methods. In particular, the fracture turning processes, during which the fracture reorients as it grows from a wellbore to become perpendicular to the minimum principal stress direction, involves viscous fluid flow and frictional slip. In addition, a moving boundary exists associated with both the fluid flow and the fracture tip. These aspects of the problem increase its complexity, but must be included in any realistic model.

In this paper, we will employ a 2D numerical method that can model hydraulic fracture growth from a borehole. The 2D plane strain assumption is justified if the height of a slot or natural flaw is large compared to the well radius. Moreover, the method can directly cope with the fracture interaction with the wellbore and natural fractures. Although the thermal effect is not yet considered, the results provide insights into fracture development around the wellbore in a hot dry rock reservoir.

PROBLEM STATEMENTS

The properties used in the model for the rock, fluid and fractures are as follows. The elastic properties for the intact rock are Young's modulus (E), Poisson's ratio (ν) and the Mode I fracture toughness is K_{IC}. The injected fluid is incompressible and has a Newtonian viscosity given by μ. The sum of all injection rates of fracture branches growing from the well is assumed to be constant and is denoted as Q_{in}. It must be noted that the injected fluid rate into each fracture varies in time because of the different growth rates of each fracture. The total rate

injected, Q_{in}, is specified as constant and represents the rate fluid is injected into the well. In addition, the volume change (compressibility) of the borehole fluid and rock system is not accounted for in determining the injection rate.

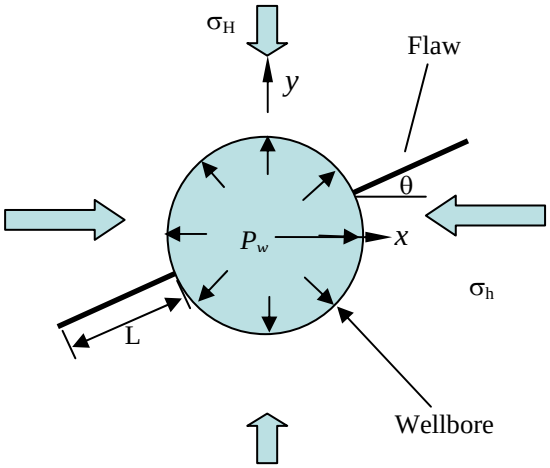

Figure 1 Fractures around a wellbore, in-situ stress and coordinate system. The origin of the coordinate system is at the wellbore centre.

The two sides of a fracture may come into contact, especially near the wellbore. The model allows for contact stresses to develop and uses a cohesionless Coulomb friction criterion for slip on surfaces in contact

$$|\tau| \le \lambda(\sigma_n - p_f) \qquad (1)$$

where τ is the shear stress along the closed fractures, σ_n is the normal stress acting across them, p_f is the fluid pressure and λ is the coefficient of friction.

In addition to the tangential displacement discontinuity (DD), *v,* associated with slip along the closed fracture segments, there exists opening displacement *w* along the opened hydraulic fractures, which contributes to fracture conductivity. All of these elastic displacements give rise to changes in the rock stress or changes in the tractions acting along the fracture surfaces. The governing equations for stresses, fluid pressure and displacements are given in Zhang et al. (2007, 2009), and are given in terms of Green's functions. We employ the displacement discontinuity method (DDM) for the simulation of rock deformation in a 2D homogeneous and isotropic elastic material, on which a uniform stress is applied at infinity.

The governing equations for fluid flow in the fracture channel are given by Zhang et al. (2009). There are two type of fluid migration along fractures. The fluid not only can diffuse along the closed fractures without any mechanical opening of the fracture, but also can flow through an open channel as a result of opening mode hydraulic fracturing processes. In the latter case, the fluid pressure is balanced by the compressive stress caused by rock elastic deformation, that is, $\sigma_n = p_f$. We use Reynolds' equation to describe fluid movement inside the opened hydraulic fractures:

$$\frac{\partial(w+\varpi)}{\partial t} = \frac{\partial}{\partial s}\left[\frac{(w+\varpi)^3}{\mu'}\frac{\partial p_f}{\partial s}\right] \qquad (2)$$

where w is the mechanical opening and vanishes for the closed segments, ϖ is the pre-existing hydraulic aperture arising from surface roughness and microstructures and $\mu' = 12\mu$.

However, it must be mentioned that effective stress changes in the fluid-infiltrated and pressurised fracture portion can produce changes of the hydraulic aperture without fully opening a fracture. The dilatation can slightly affect the internal pressure distributions since the resulting fluid conductivity varies in location and time. As stated above, the hydraulic aperture at the beginning is assigned an initial value w_0 for each closed fracture segment. The evolution of w_0 obeys a nonlinear spring model in response to any increments of the internal pressure. In particular, an equation governing the hydraulic aperture change associated with pressure change is given as follows,

$$d\varpi / dP_f = \chi\varpi \qquad (3)$$

where χ is a small constant with a value of 10^{-8} per Pa in the model. A pressure diffusion equation is applied to calculate the fluid flow inside a closed natural fracture (Zhang et al., 2009)

$$\frac{\partial p_f}{\partial t} - c\frac{\partial}{\partial s}\left(\varpi^2\frac{\partial p_f}{\partial s}\right) = 0 \qquad (4)$$

where $c = 1/(12\chi\mu)$. This calculation applies to all closed portions of fractures, whether they are undergoing or have undergone slip or not.

To complete the problem formulation, we need boundary and initial conditions for the above governing equations. Initially, all fracture segments are assumed to be evacuated and the rock mass is stationary. Rock failure criterion will be given below, as well as the method used for handling fracture intersection and associated flux redistribution. For the fractures connected to the borehole, the sum of the fluid flux entering them is equal to the injection rate, that is,

$$\sum_{i=1}^{N} q_i(0,t) = Q_{in} \qquad (5)$$

where *N* is the number of fractures and q_i the

fluid volumetric flux into fracture *i.*

At the fracture tip, the opening and shearing DDs are zero, that is,

$$w(l) = v(l) = 0 \qquad (6)$$

and the fracture opening profile near the crack tip possesses a square root shape with distance from the tip as predicted by Linear Elastic Fracture Mechanics (LEFM) theory.

When the stress intensity factor at the fracture tip reaches the fracture toughness of the rock, fracture growth occurs. In general, the fracture propagation direction may change as dictated by the near-tip stress field characterised by the Stress Intensity Factors (SIFs). In particular, the mixed-mode fracture criterion is used for determining fracture growth in the model. This same approach has been used by a number of researchers (e.g. Mogilevskaya et al., 2000).

The coupled fluid flow (to obtain pressure) and rock deformation (to obtain fracture opening) problem is solved in an implicit manner by incorporating the elasticity equation into the Reynolds' equation. The responses obtained are history dependent because of the irreversible fluid flow and frictional sliding processes. Additionally, there are three moving fronts inherent in the problem, namely the slip front, the fluid front and the fracture opening (crack tip) front. The reader is referred to Zhang et al. (2007, 2009) for a detailed description of the numerical solution methods applied in modelling these processes. At the borehole, the fracture entry pressures must be equal to the borehole pressure. This condition is enforced through an iteration scheme. The fracture entry and borehole pressures are constrained to be equal by enforcing Eq. (5). The injection rate into each fracture is found based on the specified current borehole pressure, using the method described in our previous work applied to fracture junctions (Zhang et al., 2007). In the calculation, the convergence of the solution is very sensitive to the time step and the convergence error tolerance. To rapidly find a converged wellbore pressure, a relaxation factor is used in updating the borehole pressure at each iteration step. A tolerance ($<10^{-4}$) is set for the relative error between the wellbore and fracture entry pressures. Therefore, in the program, a new iteration loop is introduced for obtaining a converged borehole and fracture entry pressure solution.

The numerical method has been verified, in our previous papers, by comparison to published solutions to a range of problems; see Zhang et al. (2009). However, to treat problems that include a borehole, the program was modified to allow correct treatment of the interior and exterior problems generated when the borehole is discretised using the DD (Displacement Discontinuity) method. Discretising the wellbore using conventional DD elements results in the formation of a disc of rock inside the wellbore, which can move rigidly. It must be mentioned that the resulting DDs along the wellbore boundary are fictitious although they are necessary for calculating pressure and displacement at the borehole wall and along the fractures. These fictitious DDs do not have a literal physical interpretation as DDs, but rather are needed to obtain the stress and displacement everywhere in the exterior part of the problem. Moreover, since the interior disc is free to move as a rigid body, the direct use of a conventional DDM is not possible without suppressing the rigid-body motion of this disc.

A simple method to suppress these rigid-body motions is as follows. Two additional elements are defined inside the borehole and assigned fictitious DDs. Then we calculate the displacement on the negative side of an element based on the fundamental elastic solutions. After that the four displacements at these two additional elements are set to zero, in order to construct a closed, well-posed problems for all DDs. The displacements on the negative side of the elements are given as Eq. (5.6.1) in Crouch and Starfield (1983) for both normal and tangential displacement components.

The elasticity equations for the normal and tangential DDs (Δu_k includes *w* and *v*.) at the middle of each element along the borehole and the fractures and for the two additional elements are, respectively,

$$K_{ijk}\Delta u_k = P_f \delta_{ij} - \sigma_{ij}^{\infty} \qquad k = n, s \qquad (7)$$

$$M_{ijk}\Delta u_k = 0 \qquad k = n, s \qquad (8)$$

where K_{ijk} and M_{ijk} are the coefficient matrices derived from the fundamental elastic solution as is done in conventional boundary element methods (see details in Crouch and Starfield, 1983); and σ_{ij}^{∞} are the resultant stresses along the fracture surface arising from far-field (in situ) stresses.

The above first equation enforces equilibrium at DD elements along the fractures and the wellbore, and the second one enforces the constraint that eliminates rigid body motion of the interior disc by requiring zero displacements at two additional interior elements. The above simultaneous equations (Eqns (7) and (8)) are solved for normal and shear DDs of all elements along the borehole, the fractures and of the two additional elements, once the fluid pressure is known. The DDs that are obtained can then be used to calculate stress or displacement at any other point inside the rock mass.

NUMERICAL RESULTS

Single hydraulic fracture

We first compare the opening and path for a hydraulic fracture driven by a uniform pressure or by injection of a viscous fluid. A uniform pressure condition in a hydraulic fracture is equivalent to using an inviscid fluid (Detournay, 2004). The pressure magnitude is adjusted at each fracture growth step to satisfy the fracture extension criterion at the fracture tip. Fracture reorientation is clearly shown in Fig. 2 for both uniformly pressurised and viscous fluid flow cases. For zero viscosity fluids as shown in Fig. 2(a), the portion adjacent to the well wall is in contact. In this region, fluid flow will be restricted and frictional slip condition must be imposed. For generality of results, Mogilevskaya et al. (2000) showed that the fracture path is controlled by the following dimensionless parameter,

$$\beta = \frac{(\sigma_H - \sigma_h)\sqrt{R}}{K_{IC}} \qquad (9)$$

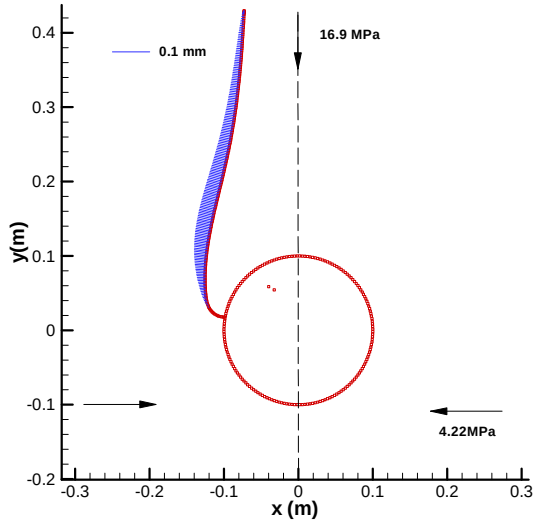

(a)

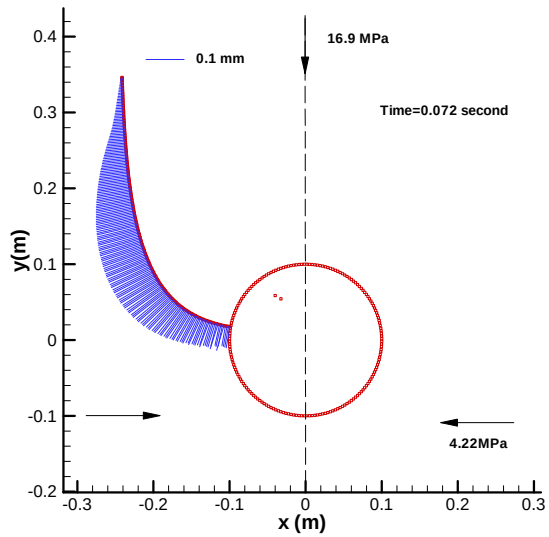

(b)

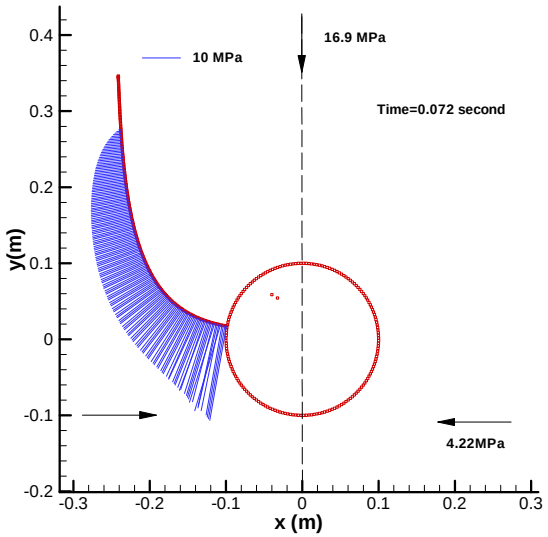

(c)

Figure 2 Fracture trajectory, opening DD for uniformly pressurised fractures (a); opening DD (b) and internal fluid pressure (c) for fluid-driven fracture growth in the case of the borehole radius =0.1 m and crack starting angle of 170 degree.

If the fluid viscosity is 0.01 Pa s and the injection rate is specified as 0.0004 m^2/s, the fracture pathway and associated opening DD and pressure distributions are given in Figs. 2(b) and (c). The fracture closure does not appear in this case, but a high fluid pressure results as the fluid enters the narrow fracture and opens it against the higher normal stresses acting along its near well extent Fig. 2(c). Moreover, a fluid lag zone develops when viscous dissipation cannot be neglected and is represented in Fig. 2(c) as the unpressurised region of the fracture near the tip. This is one manifestation of the coupled flow and deformation process interacting with a moving boundary.

To characterize the effect of fluid viscous dissipation on fracture paths, we introduce another parameter which provides an apparent fracture toughness arising from viscous dissipation, as given in Jeffrey(1989), based on an earlier somewhat different formulation given by Settari and Price (1984), and as given by Detournay (2004) in the case of zero lag. This apparent toughness, when substituted for the rock fracture toughness in Eqn. 9 provides a dimensionless parameter, given by Eqn. 10, that we hypothesize will control the curving of a viscosity dominated hydraulic fracture growing from a wellbore (Zhang et al. 2010),

$$\chi_F = \frac{(\sigma_H - \sigma_h)\sqrt{R}}{(\mu' Q_{in} E'^3)^{1/4}} \qquad (10)$$

where E' is the plane-strain modulus. In this formula, the product of injection rate Q_{in} and fluid

viscosity μ are parameters that can be controlled by a fracturing engineer.

The above two parameters given by Eqs. (9) and (10) can fully characterise the fracture path and related pressure evolution for a single hydraulic fracture growing from a wellbore. Zhang et al. (2010) provide numerical examples demonstrating that these parameters control the curvature in the hydraulic fracture path as it grows from an uncased wellbore.

Two winged hydraulic fractures

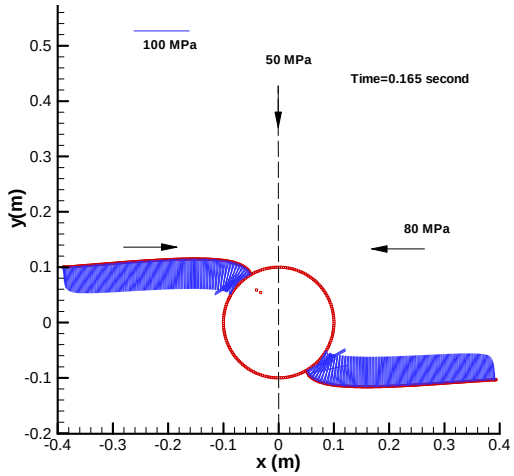

Figure 3 A pair of fractures growing from a wellbore: fracture trajectory and internal fluid pressure for high-angle fracture initiation. The fluid viscosity is 0.01 Pa s and the injection rate is specified as 0.0004 m^2/s.

We next consider two fractures that grow simultaneously to form a single bi-wing fracture geometry as shown in Fig. 3. The pressure loss near the wellbore wall is less evident and fracture rotation to align with the maximum principal stress occurs in a very smooth way. This symmetric geometry is found in many field observations as described by Weng (1993) and Cherny et al. (2009).

Multiple hydraulic fractures

The more complicated initial condition consisting of six starter fractures that are arranged around the wellbore is considered next. The starter fractures have an uneven angular distribution to the x-axis of 30°, 120°, 150°, 210°, 240° and 330°, as shown in Fig. 4. The fractures at angles of 120° and 240° are in a more compressive initial stress state, which causes their growth to be completely suppressed compared with other four fractures. The remaining four starter fractures are all subjected to the same stress levels, except for the shear stress directions. The fracture at angle 150° is can extend more easily because it has a slightly longer initial fracture length. As the fractures grow and turn to align with the horizontal x direction, the fractures at the angle of 150° and 330° become more dominant and form a bi-wing fracture configuration. However, the other two fractures at angle 30° and 210°, do extend but to a shorter distance. These two fractures propagate towards the longer fractures after leaving the influence region around the borehole and a sharp kink is evident in Fig. 4. The tendency for fracture linkage is also clear. The slowly growing and partially suppressed fractures propagate towards the dominant growing fractures and may link-up with them as previously found by Weng (1993). These results suggest that initiation of several fractures from a wellbore subject to a larger stress ratio favours interactions leading to link-up as argued by Daneshy (1973).

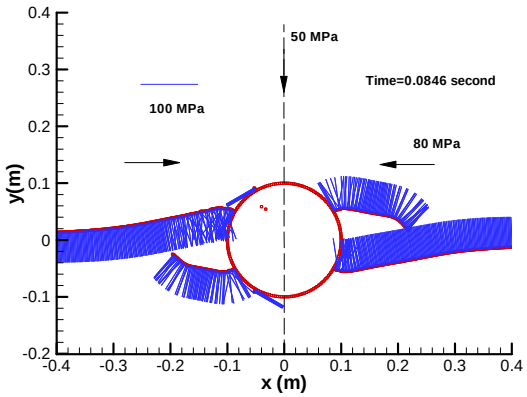

Figure 4 Fracture trajectory and internal fluid pressure in the presence of six initial flaws around the wellbore, where the fluid viscosity is 0.005 Pa s and the injection rate is specified as 0.0012 m^2/s. The flaw alignment angles are 30°, 120°, 150°, 210°, 240° and 330°.

Effects of natural fractures

If there is a natural fracture in the fracture propagation pathway, fluid will enter it after a hydraulic fracture intersects it. The existence of natural fracture will affect the growth of the hydraulic fracture and the inflation of the natural fracture caused by the fluid pressure can induce slip along the natural fracture and fracture reinitiation from the ends of a finite-size natural fracture. The example fracture geometry is given in Fig. 5(a).

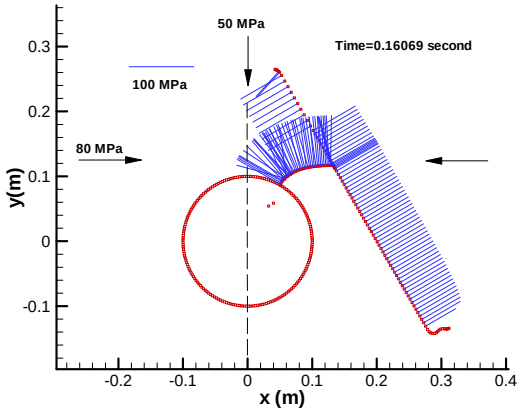

(a)

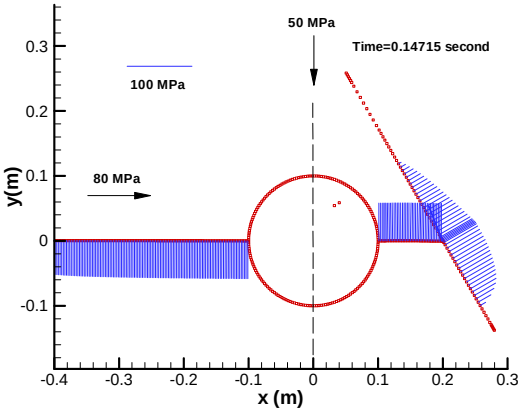

(b)

Figure 5 Fracture trajectory and internal fluid pressure in the presence of a natural fracture that has finite length and an inclination angle of 135 degree with respect to the x-axis. The coefficient of friction of the natural fracture is 0.3. The fluid viscosity is 0.01 Pa s and the injection rate is specified as 0.0004 m^2/s.

The arrest of one fracture will facilitate the propagation of a second wing of a two-winged fracture, as shown in Fig. 5(b). The left-hand side fracture propagates at a lower pressure, taking most of injected fluid and growing much faster.

References

Abass, H. H., Soliman, M. Y., Tahini, A. M., Surjaatmadja, J., Meadows, D. L., Sierra, L., 2009, Oriented fracturing: A new technology to hydraulically fracture openhole horizontal well, SPE 124483, Proceedings of the 2009 SPE Annual Technical Conference and Exhibition, New Orleans, Louisiana, October 4-7 2009

Cherny, S., Chirkov, D., Lapin, V., Muranov, A., Bannkov, D., Miller, M., Willberg, D., Medvedev, O. and Alekseenko, O., 2009, Two-dimensional modelling of the near-wellbore fracture tortuosity effect, Int. J. Rock Mech. & Mining Sci. 46, p. 992-1000.

Crouch, S. L. and Starfield, A. M., 1990, Boundary Element Method in Solid Mechanics, Unwin Hyman, Boston

Daneshy, A. A., 1973, A study of inclined hydraulic fractures, SPE J 13: p. 61-68.

Detournay, E., 2004, Propagation regime of fluid-driven fractures in impermeable rocks, Int. J. Geomechanics 4, p. 35-45.

Detournay, E. and Jeffrey, R., 1986, Stress conditions for initiation of secondary fractures from a fractured borehole, proceedings of the international symposium on rock stress and rock stress measurements, Stockholm, Sweden, 1-3, September, 1986.

Hamison, B. and Fairhurst C., 1970 In-situ stress determination at great depth by means of hydraulic fracturing, in Rock Mechanics—Theory and Practice, (ed.) W. H. Somerton, Am. Inst. Mining Engrg., 559–584, 1970

Jeffrey, R. G., 1989 The combined effect of fluid lag and fracture toughness on hydraulic fracture propagation, SPE 18957, Proceedings of SPE Joint Rocky Mountain Regional/ Low Permeability Reservoirs Symposium and Exhibition, Denver, Colorado, March 6-8, 1989.

Manrique, J.F. and Venkitaraman, A., 2001, Oriented fracturing – A practical technique for production optimization, Proceedings of the 2001 SPE Annual Technical Conference and Exhibition held in New Orleans, Louisiana, 30 September–3 October 2001

Mogilevskaya, S. G., Rothenburg, L. and Dusseault, M. B., 2000, Growth of pressure-induced fractures in the vicinity of a wellbore, International Journal of Fracture 104, p. L25-L30.

Settari, A. and H. S. Price., 1984, Simulation of hydraulic fracturing in low-permeability reservoirs, SPEJ April 1984, p. 141-152.

Soliman, M. Y., East, L. and Adams, D., 2008, Geomechanics aspects of multiple fracturing of horizontal and vertical wells, SPE 86889, SPE Drilling and Completion, Sept. 2008, 217-228.

Weng, X., 1993, Fracture Initiation and Propagation from Deviated Wellbores, SPE 26597, presented at the 1993 ATCE, Houston, TX, 3-6 October, 1993.

Zhang, X. Jeffrey, R. G. and Thiercelin, M., 2007, Deflection of fluid-driven fractures at bedding interfaces: A numerical investigation, J. Structural Geology 29, p. 396-410.

Zhang, X. Jeffrey, R. G. and Thiercelin, M., 2009, Mechanics of fluid-driven fracture growth in naturally fractured reservoirs with simple network geometries, J. Geophysical Research -Solid Earth, 114, B12406.

Zhang, X. Jeffrey, R.G., Bunger, A.P. and Thiercelin, M., 2010 Initiation and growth of a hydraulic fracture from a borehole under toughness- or viscosity- dominated conditions, 44th US Rock Mechanics Symposium and 5th U.S.-Canada Rock Mechanics Symposium, Salt Lake City, UT June 27–30, 2010.